

Mechanism-Based Inactivation of Human Cytochrome P450 3A4 by Two Piperazine-Containing Compounds[§]

Amanda K. Bolles, Rina Fujiwara, Erran D. Briggs, Amin A. Nomeir, and Laura Lowe Furge

Amin Nomeir Pharmaceutical Consulting, LLC, Milford, New Jersey (A.A.N.); and Department of Chemistry, Kalamazoo College, Kalamazoo, Michigan (A.K.B., R.F., E.D.B., L.L.F.)

Received August 26, 2014; accepted October 1, 2014

ABSTRACT

Human cytochrome P450 3A4 (CYP3A4) is responsible for the metabolism of more than half of pharmaceutical drugs, and inactivation of CYP3A4 can lead to adverse drug-drug interactions. The substituted imidazole compounds 5-fluoro-2-[4-[(2-phenyl-1*H*-imidazol-5-yl)methyl]-1-piperazinyl]pyrimidine (SCH 66712) and 1-[[2-ethyl-4-methyl-1*H*-imidazol-5-yl)methyl]-4-[4-(trifluoromethyl)-2-pyridinyl]piperazine (EMTPP) have been previously identified as mechanism-based inactivators (MBI) of CYP2D6. The present study shows that both SCH 66712 and EMTPP are also MBIs of CYP3A4. Inhibition of CYP3A4 by SCH 66712 and EMTPP was determined to be concentration, time, and NADPH dependent. In addition, inactivation

of CYP3A4 by SCH 66712 was shown to be unaffected by the presence of electrophile scavengers. SCH 66712 displays type I binding to CYP3A4 with a spectral binding constant (K_S) of $42.9 \pm 2.9 \mu\text{M}$. The partition ratios for SCH 66712 and EMTPP were 11 and 94, respectively. Whole protein mass spectrum analysis revealed 1:1 binding stoichiometry of SCH 66712 and EMTPP to CYP3A4 and a mass increase consistent with adduction by the inactivators without addition of oxygen. Heme adduction was not apparent. Multiple mono-oxygenation products with each inactivator were observed; no other products were apparent. These are the first MBIs to be shown to be potent inactivators of both CYP2D6 and CYP3A4.

Introduction

Cytochrome P450 enzymes (P450s) are a family of heme-containing proteins involved in the metabolism of small endogenous and exogenous compounds in humans (Guengerich, 2003). One major class of substrates for P450s is pharmaceutical drugs. Among drug-metabolizing P450 enzymes, CYP3A4 participates in the metabolism of up to 50% of marketed drugs and has high protein expression in liver (~30% of total P450 content) and small intestine (Guengerich, 2003). CYP2D6, another less abundant drug metabolizing P450, metabolizes ~15% of pharmaceuticals and is expressed at much lower levels (~2-5% of total P450 content; Guengerich, 2003). Together, CYP3A4 and CYP2D6

metabolize nearly three quarters of pharmaceutical drugs. Substrates for CYP2D6 tend to contain basic nitrogens and aromatic rings and include many pharmaceuticals with narrow therapeutic indices such as antihypertensives and psychoactive drugs (Guengerich, 2005). CYP3A4 has a broader substrate specificity and metabolizes drugs from many diverse groups including antimicrobials, androgens, anticancer agents, anti-HIV agents, and plant alkaloids (e.g., St. John's Wort; Guengerich, 2005). Given their important roles in drug metabolism, inhibition or inactivation of CYP3A4 or CYP2D6 can lead to adverse drug events, particularly in cases of polypharmacy.

Structurally, both CYP3A4 and CYP2D6 show the characteristic P450-fold with helices A-L, some beta sheets, and the heme iron hexacoordinated to the porphyrin ring nitrogens, the proximal cysteine sulfur, and water on the distal side (in the absence of substrate). One striking difference, however, is the binding cavity size. CYP3A4 has approximately more than double the binding cavity size of CYP2D6 (~1560 Å³ versus ~540 Å³, respectively) (Ekroos and Sjogren, 2006; Rowland et al., 2006). The difference in binding cavity has been offered as an explanation for the CYP3A4 greater substrate promiscuity as well as observed cooperativity (Ekroos and Sjogren, 2006).

One disadvantage of broad substrate specificity is the susceptibility of P450 enzymes to inhibition by covalent inactivation by compounds being metabolized (Correia and Ortiz de Montellano, 2005). This type of inhibition is known as mechanism-based inactivation (MBI) and the loss of enzyme activity can be by covalent adduction of the protein, the heme, or by cross reaction of heme and protein (Hollenberg et al., 2008). Because inactivation is not reversible, MBIs are an important

This work was supported by the National Institutes of Health National Institute of General Medical Sciences [Grant 1R15-GM086767-02] (to L.L.F.); a grant to Kalamazoo College from the Howard Hughes Medical Institute [52006304] through the Precollege and Undergraduate Science Education Program; and the Cook, Hutchcroft, and Varney Funds of Kalamazoo College.

A.K.B. and R.F. contributed equally to this work.

Part of this work was previously presented as follows: Fujiwara R, Bolles A, and Furge L (2014) Mechanism-based inactivation of human CYP3A4 by a piperazine-containing compound. *Experimental Biology* 2014; 2014 April 26-30, San Diego, CA. American Society for Biochemistry and Molecular Biology, Rockville, MD.

Bolles A, Nomeir A, and Furge L (2014) 5-Fluoro-2-[4-[(2-phenyl-1*H*-imidazol-5-yl)methyl]-1-piperazinyl]pyrimidine is a mechanism based inactivator of CYP3A4. *Experimental Biology* 2014; 2014 April 26-30, San Diego, CA. American Society for Biochemistry and Molecular Biology, Rockville, MD.

dx.doi.org/10.1124/dmd.114.060459.

[§]This article has supplemental material available at dmd.aspetjournals.org.

ABBREVIATIONS: ACN, acetonitrile; AMG 487, (*R*)-*N*-{1-[3-(4-ethoxy-phenyl)-4-oxo-3,4-dihydro-pyrido[2,3-*d*]pyrimidin-2-yl]-ethyl}-*N*-pyridin-3-yl-methyl-2-(4-trifluoromethoxy-phenyl)-acetamide; EMTPP, 1-[[2-ethyl-4-methyl-1*H*-imidazol-5-yl)-methyl]-4-[4-(trifluoromethyl)-2-pyridinyl]piperazine; ESI, electrospray ionization; HPLC, high-performance liquid chromatography; LC, liquid chromatography; MBI, mechanism-based inactivation; MS, mass spectrometry; NAC, *N*-acetyl cysteine; P450, cytochrome P450; SCH 66712, 5-fluoro-2-[4-[(2-phenyl-1*H*-imidazol-5-yl)methyl]-1-piperazinyl]pyrimidine; TFA, trifluoroacetic acid.

class of inhibitors to consider when studying drug-drug interactions involving P450 enzymes. There are many known MBIs of CYP3A4 including raloxifene, bergamottin, lapatinib, 4-ipomeanol, mifepristone, 17 α -ethynylestradiol, and erythromycin (He et al., 1998; Chen et al., 2002; Lin et al., 2002; Alvarez-Diez, 2004; Zhou et al., 2005; Baer et al., 2007; Yukinaga et al., 2007; Teng et al., 2010). Many of these inactivators form covalent adducts with CYP3A4 at amino acids, such as raloxifene and AMG 487 [(*R*)-*N*-{1-[3-(4-ethoxy-phenyl)-4-oxo-3,4-dihydro-pyrido[2,3-*d*]pyrimidin-2-yl]-ethyl}-*N*-pyridin-3-yl-methyl-2-(4-trifluoromethoxy-phenyl)-acetamide] adduct at Cys239 whereas bergamottin adducts at Gln273 (Baer et al., 2007; Henne et al., 2012; Lin et al., 2012).

In contrast to CYP3A4, for CYP2D6 only a few inactivators are established, and of those only two are known protein adductors, SCH 66712 [5-fluoro-2-[4-[(2-phenyl-1*H*-imidazol-5-yl)methyl]-1-piperazinyl]pyrimidine] and EMTTP [1-[(2-ethyl-4-methyl-1*H*-imidazol-5-yl)-methyl]-4-[4-(trifluoromethyl)-2-pyridinyl]piperazine] (Fig. 1) (Hutzler et al., 2004; Nagy et al., 2011; Livezey et al., 2012). Amino acid sites of adduction on CYP2D6 are still unknown. SCH 66712 was discovered as a human dopamine receptor D4 antagonist, but, due to inactivation of CYP2D6, it was dropped as a lead compound (Palamanda et al., 2001). Initial studies of SCH 66712 interaction with P450 enzymes suggested that CYP3A4 would also be susceptible to inactivation by SCH 66712 (Palamanda et al., 2001). Given that EMTTP, which has no known pharmaceutical activity, is structurally similar to SCH 66712 and has previously been shown to inactivate CYP2D6, we considered that it might be an inactivator of CYP3A4 as well. Therefore the current study sought to evaluate possible inactivation of CYP3A4 by these two related CYP2D6 inactivators. To our knowledge, there are no compounds reported to be dual potent inactivators of both CYP3A4 and CYP2D6.

Materials and Methods

Chemicals. SCH 66712 was obtained from Schering-Plough Research Institute (now Merck & Co., Kenilworth, NJ) and reconstituted in water for use in assays described below. Ultrapure solvents (water, acetonitrile [ACN], and methanol) for mass spectrometry (MS) were purchased from EMD Chemicals (Gibbstown, NJ). EMTTP was purchased from Interchim (San Pedro, CA). All other solvents were high-performance liquid chromatography (HPLC) grade and purchased from Sigma-Aldrich (St. Louis, MO). Glutathione was purchased from Cayman Chemicals (Ann Arbor, MI). Potassium phosphate, *N*-acetylcysteine, NADPH, L- α -diluroyl-phosphocholine phospholipids, ACN, testosterone, 6 β -hydroxytestosterone, catalase, TiCl₃, and all other reagents were purchased from Sigma-Aldrich.

Enzymes. Recombinant human CYP3A4 was used for spectral analysis and binding titrations, and whole protein MS after purification from *Escherichia*

coli as previously described elsewhere (Gillam et al., 1993, 1995). Recombinant P450 NADPH-reductase and rabbit cytochrome *b*₅ were purified from *E. coli* as previously described elsewhere (Shen et al., 1989; Holmans et al., 1994) and were a generous gift from Dr. F. P. Guengerich, Vanderbilt University (Nashville, TN) (used for reconstitution with purified CYP3A4 as described later). For all other experiments, human CYP3A4 coexpressed with P450 reductase and cytochrome *b*₅ (Supersomes) were used (BD-Gentest, Woburn, MA).

Spectral Binding Titrations. Spectral binding titrations studies were performed with recombinant purified CYP3A4 (1 μ M) in potassium phosphate buffer (100 mM, pH 7.4). The solution was evenly divided between two cuvettes, and the experiments were performed at room temperature using a Cary 300 dual-beam spectrophotometer (Varian, Walnut Creek, CA). A baseline correction was recorded (350–500 nm). SCH 66712 (1–300 μ M) was then titrated into the sample cuvette, and the equivalent volume of water was added to the reference cuvette; the spectra were recorded (350–500 nm) after each addition. The difference between the absorbance maximum and minimum was plotted against SCH 66712 concentration, and the data were analyzed by a nonlinear regression using KaleidaGraph (Synergy Software, Reading, PA). The dissociation constant, K_s , was determined using the following quadratic velocity equation:

$$[\text{CYP3A4} \bullet \text{SCH 66712}] = 0.5 (K_s + E_t + S_t) - [0.25 (K_s + E_t + S_t)^2 - E_t S_t]^{1/2}$$

where S_t represents substrate concentration, E_t is the total enzyme concentration, and K_s is the spectral dissociation constant for the reaction CYP3A4 + SCH 66712 \leftrightarrow [CYP3A4•SCH 66712].

Time-Dependent Inactivation. Primary reaction mixtures containing SCH 66712 (16 μ M) or EMTTP (15 μ M), CYP3A4 Supersomes (20 pmol), and potassium phosphate buffer (100 mM, pH 7.4, in a final volume of 100 μ l) were preincubated in a 37°C shaking water bath for 3 minutes, and then all reactions except control were initiated with NADPH (1 mM). Aliquots (10 μ l) of the primary reaction were transferred after incubations of 0–30 minutes to secondary reactions (in triplicate) containing NADPH (1 mM), testosterone (100 μ M), and potassium phosphate buffer (100 mM, pH 7.4; final volume 200 μ l). Secondary reactions were incubated for 10 minutes then quenched with dichloromethane (800 μ l) and vortexed.

Product extraction was as previously reported elsewhere (Sohl et al., 2009). Briefly, a 400- μ l aliquot of 0.3 M NaCl solution was added to the sample, the samples were vortexed, and then they were centrifuged for 10 minutes at 3000g. The bottom organic layer of the sample was moved to a small glass vial, and the upper aqueous layer was disposed of. The organic layer was evaporated under a nitrogen stream. The extracted testosterone and 6 β -hydroxytestosterone were dissolved in 35 μ l of methanol.

A 10- μ l aliquot of sample was directly injected onto a Waters Symmetry C18 column (5 μ m, 3.9 \times 150 mm) connected to a Waters Alliance e2695 HPLC system with flow rate of 0.8 ml/min (Waters Corporation, Milford, MA). The mobile phase was a gradient elution with initial conditions of 78% A [95% ammonium acetate (10 mM), 5% ACN] and 22% B [1% ammonium acetate (10 mM), 99% ACN]. After 5 minutes at initial conditions, a linear gradient of 78% A to 64% A over 7 minutes was initiated followed by a hold for 8 minutes at 64% A. The gradient finished with a final decrease to 20% A over 8 minutes. After an additional 8 minutes at 20% A, the system was returned to the initial conditions. 6 β -Hydroxytestosterone and testosterone eluted at approximately 6 and 18 minutes, respectively. The ratio of 6 β -hydroxytestosterone to testosterone was quantified by HPLC and converted to percentage of remaining activity by comparing each sample ratio to the 0-minute control. The percentage of remaining activity was plotted against the primary reaction incubation time.

Concentration-Dependent Inactivation. Primary reaction mixtures with a final volume of 100 μ l containing varying concentrations of SCH 66712 (0–40 μ M) or EMTTP (0–100 μ M), CYP3A4 Supersomes (20 pmols), and potassium phosphate buffer (100 mM, pH 7.4) were preincubated in a 37°C shaking water bath for 3 minutes, and then all reactions except control were initiated with NADPH (1 mM). After 20 minutes, 10- μ l aliquots of the primary reactions were transferred to the secondary reactions (in triplicate), and the samples were incubated, extracted, and analyzed as described previously.

Trapping Agents. Primary reaction mixtures containing SCH 66712 (16 μ M), CYP3A4 Supersomes (20 pmols), and potassium phosphate buffer (100 mM,

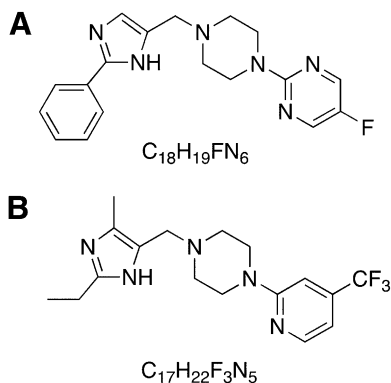


Fig. 1. Structure of SCH 66712 and EMTTP. Both compounds contain substituted imidazole rings and piperazine rings.

pH 7.4; 100 μ l final volume) were prepared as follows: with or without NADPH (1 mM final), with NADPH and glutathione (10 mM final), with NADPH and *N*-acetyl cysteine (NAC, 10 mM final), with NADPH and superoxide dismutase (SOD) (1.0 unit/ μ l final), with NADPH and catalase (0.05 μ g/ μ l final), and with NADPH and potassium cyanide (KCN, 2 mM final). Primary reactions were preincubated for 3 minutes and then initiated with NADPH (1 mM), except the no-NADPH control reaction that received an equal volume of water. Aliquots (10 μ l) of the initiated primary reaction were removed and added to the secondary reactions at 0 and 12 minutes of incubation (final volume 200 μ l), and samples were treated, extracted, and analyzed as described previously. The effect of each variable on inhibition was determined by comparing the percentage of remaining activity after 12 minutes of the no-NADPH control with the NADPH reactions.

Partition Ratio. Primary reaction mixtures contained CYP3A4 Supersomes (20 pmols), potassium phosphate buffer (100 mM, pH 7.4), and varying concentrations of SCH 66712 (0–40 μ M) or EMTTP (0–80 μ M) in a final volume of 100 μ l. The primary reaction mixtures were preincubated in a shaking water bath at 37°C for 3 minutes, and then all primary reactions except the control were initiated with NADPH (1 mM). The control received an equal volume of water. The primary reactions were then incubated for 30 minutes to ensure inactivation was complete. Aliquots of 10 μ l were added to the secondary reactions, and the samples were incubated, extracted, and analyzed as described previously. The ratio of 6 β -hydroxytestosterone to testosterone was converted to percentage of remaining activity by comparing each sample to the zero concentration control. From a plot of the percentage of remaining activity versus [inactivator]/[CYP3A4], the partition ratio was calculated by the method of Silverman using the intersection of the linear regression of the steeper slope of the high ratios with the *x*-axis (Silverman, 1988).

Determination of K_1 and k_{inact} . Primary reactions with a final volume of 100 μ l containing varying concentrations of SCH 66712 (0–16 μ M) or EMTTP (0–40 μ M), CYP3A4 Supersomes (20 pmols), and potassium phosphate buffer (100 mM, pH 7.4) were preincubated in a 37°C shaking water bath for 3 minutes, and then all reactions were initiated with NADPH (1 mM). Aliquots (10 μ l) of the primary reaction were transferred after 0 to 30 minutes of incubation (0, 1, 2, and 5 minutes in reactions with SCH 66712 and 0, 10, 20, and 30 minutes in reactions with EMTTP) to the secondary reactions (in triplicate), and the samples were incubated, extracted, and analyzed as described previously. The log of the percentage of remaining activity was plotted against incubation time for each concentration. The initial rates of inactivation (k_{obs}) were then plotted against the concentration of inactivator and fit by nonlinear regression [$k_{obs} = (k_{inact}[\text{inactivator}])/(K_1 + [\text{inactivator}])$] to determine k_{inact} and K_1 using KaleidaGraph (Synergy Software, Reading, PA).

Native Heme Analysis by HPLC. Analysis of heme was as previously described with the following modifications (Nagy et al., 2011). Four reaction mixtures were used: controls containing no SCH 66712 and no NADPH, no SCH 66712 with NADPH (1 mM, final), or SCH 66712 (16 μ M) without NADPH, and one experimental with SCH 66712 (16 μ M) with NADPH (1 mM, final). Each reaction included CYP3A4 Supersomes (20 pmol) in potassium phosphate buffer (100 mM, pH 7.4; final volume 80 μ l). Reactions were preincubated in a 37°C shaking water bath for 3 minutes before initiation by the addition of NADPH (1 mM final); an equal volume of water was added to the no-NADPH controls.

After 0, 3, 5, 10, and 15 minutes, the reactions were quenched by the addition of 10 μ l of ACN, and the samples were placed on ice. For heme adduct analysis, incubation mixtures were injected onto a PROTO 300, C₄, 5 μ m, 2.1 \times 250 mm column connected to a Waters Alliance e2695 HPLC system, and the mobile phase was a gradient elution with initial conditions of 70% A (0.1% trifluoroacetic acid [TFA] in H₂O) and 30% B (0.05% TFA in ACN) that was ramped linearly to 20% A over 30 minutes, and then returned to the initial conditions. Heme was monitored using a Waters model 2487 dual wavelength UV/Vis detector at 405 nm. Heme eluted at ~22.5 minutes.

Liquid Chromatography Electrospray Ionization Mass Spectrometry Analysis of CYP3A4. Purified, recombinant CYP3A4 (100 pmols; 1 μ M) was reconstituted with reductase (3 μ M), cytochrome *b*₅ (2 μ M), and freshly sonicated L- α -dilauroyl-phosphocholine phospholipids (30 μ M) at room temperature for 10 minutes. Then potassium phosphate buffer (pH 7.4, 100 mM) was added along with SCH 66712 (100 μ M in water) or EMTTP (75 μ M in methanol not exceeding 1% final v/v of solvent). Control reactions without

SCH 66712 or EMTTP received water or methanol, respectively. Reactions were incubated for an additional 3 minutes at 37°C and then initiated by the addition of NADPH (1 mM) or water in the no-NADPH controls. Final reaction volumes were 100 μ l. After 15 minutes (reactions with SCH 66712) or 30 minutes (reactions with EMTTP), samples were immediately analyzed by liquid chromatography electrospray ionization mass spectrometry (LC-ESI-MS). Reaction of CYP3A4 with iodoacetamide was performed as a validation for the assay as previously described elsewhere (Baer et al., 2007).

For LC-ESI-MS analysis, an aliquot of each reaction (20 μ l, 20 pmol) was directly injected on to a reversed-phase PROTO 300 C₄ column, 5 μ m, 2.1 \times 250 mm, and chromatographic separation was performed using an Alliance Waters 2690 HPLC system (Waters Corporation). The solvent system consisted of A (0.1% TFA in water) and B (0.1% TFA in ACN). A flow rate of 0.2 ml/min was used. After an initial 5-minute hold at 100% A, a linear gradient of 100% A to 10% A over 35 minutes was applied for resolution of protein components followed by a 10-minute hold at 10% A and then returned to the initial conditions. The column effluent starting at 10 minutes was directed into an LXQ mass analyzer operated in the positive ion mode and using the Xcalibur software package (Thermo Fischer Scientific, Waltham, MA). The system had been optimized with horse heart myoglobin. The ESI conditions were sheath gas, 20 arbitrary units; auxiliary gas, 9 arbitrary units; spray voltage, 5 kV; capillary temperature, 275°C; capillary voltage, 48 V; and tube lens offset, 120 V. The molecular masses of CYP3A4 were determined by deconvolution of the apoprotein charge envelopes using ProMass software (Novatia, LLC, Mammouth Junction, NJ).

Metabolite Analysis. We previously reported the metabolites of SCH 66712 formed by P450s 2D6, 2C9, and 2C19 (Nagy et al., 2011). In similar metabolism experiments with CYP3A4, mono-oxygenation of SCH 66712 at four different positions was apparent by the presence of four distinct *m/z* 355 ions in the mass spectral analysis (M+1). To determine whether mono-oxygenation was on carbon or nitrogen atoms, titanium trichloride (TiCl₃) was used to selectively reduce any hydroxylamines as previously described elsewhere (Seto and Guengerich, 1993; Kulanthaivel et al., 2004; Livezey et al., 2014). Because the metabolites formed by CYP3A4 and by CYP2D6 were the same, the metabolites as formed by CYP2D6 were used in the TiCl₃ experiments due to the more uniform distribution of products (as compared with CYP3A4) and therefore ease of comparison of changes upon HCl or TiCl₃ treatment (vide infra).

Briefly, reaction mixtures containing SCH 66712 (100 μ M) and CYP2D6 Supersomes (150 pmol) in potassium phosphate buffer (100 mM, pH 7.4; final volume 600 μ l) were initiated by the addition of NADPH (1 mM). Reactions were incubated at 37°C for 30 minutes and then analyzed. One aliquot (200 μ l) of the reaction mixture was treated with 30 μ l of a solution of TiCl₃ (~10 wt. % in 20–30 wt. % HCl). For controls, one aliquot (200 μ l) was treated with HCl alone (25 wt %) and another aliquot (200 μ l) was left untreated. Samples were left at room temperature for 1 hour to allow for TiCl₃ reduction of hydroxylamines to the parent amines. A control sample not treated with TiCl₃ or HCl was placed on ice for 1 hour. All samples were then centrifuged, and the supernatant was analyzed by LC-ESI-MS as described previously (Nagy et al., 2011; Livezey et al., 2014).

Metabolites of EMTTP formed by CYP3A4 were determined by LC-ESI-MS using the methods described previously with SCH 66712 with modification (Nagy et al., 2011). Briefly, CYP3A4 Supersomes were incubated for 45 minutes with EMTTP (100 μ M) and NADPH (1 mM) in potassium phosphate (pH 7.4, 100 mM) and final volume of 100 μ l. Reactions were terminated with 30 μ l ACN. Samples were centrifuged and the supernatant (20 μ l) injected directly on to a Kinetix C18 (2.5 μ m, 2.1 \times 100 mm) column (Phenomenex, Torrance, CA) for chromatographic separation and MS analysis using conditions previously described elsewhere (Nagy et al., 2011). TiCl₃ treatment of EMTTP metabolites as formed by CYP3A4 was performed as described earlier with SCH 66712 metabolites.

Site of Metabolism Predictions. The software programs SMARTCyp (Rydberg et al., 2010; Rydberg and Olsen, 2012) and RS-Predictor (Zaretski et al., 2012) were used for prediction of sites of metabolism on SCH 66712 by CYP3A4 and by other P450s.

Molecular Modeling and Docking Simulations. AutoDock Vina was employed for docking simulations and molecular modeling (<http://autodock.scripps.edu>; Morris et al., 1998; Huey et al., 2007). The protein structure used in these

studies was CYP3A4 complexed with ritonavir (PDB ID: 3NXU) (Sevrioukova and Poulos, 2010). Ritonavir and solvent molecules were removed, but the heme was retained. A water molecule was placed 1.7 Å from the heme iron using COOT (Emsley and Cowtan, 2004) to simulate the electrostatics of Compound I in the mechanism of P450 catalysis (Shahrokhi et al., 2012). Charges were calculated by the Gasteiger-Marsili method. The three-dimensional structures of the ligands for docking studies were built in Spartan 4.0 (Wavefunction, Irvine, CA) with all hydrogen atoms added and energy minimization. The dimensions of the grid box were set to 18 × 18 × 18 Å and the grid spacing was set to 1.0 Å. The consensus binding postures of the molecules were obtained by visual inspection and docking scores.

Results

Inactivators. SCH 66712 and EMTTP are structurally similar molecules both containing piperazine rings and substituted-imidazole rings as well as heteroaromatic rings with fluorine substituents. Although SCH 66712 is a human dopamine receptor antagonist, no pharmaceutical activity has been noted for EMTTP (Fig. 1).

Spectral Binding with SCH 66712. SCH 66712 displayed type I substrate binding upon titration with CYP3A4 (Fig. 2A). Fit of the binding data with the quadratic equation yielded a K_s of $42.9 \pm 2.9 \mu\text{M}$ (Fig. 2B).

Time- and Concentration-Dependent Inactivation of CYP3A4 by SCH 66712 and EMTTP. Treatment of CYP3A4 in time- and

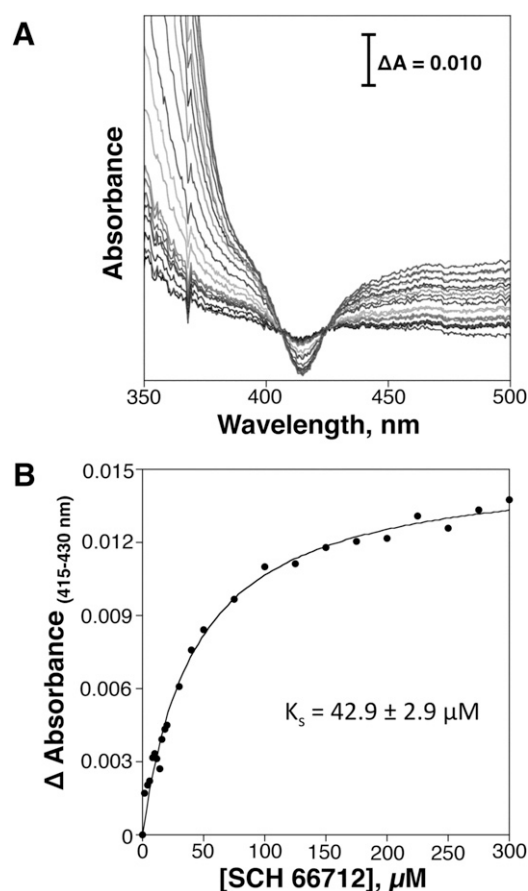


Fig. 2. Spectral binding titration of SCH 66712 with CYP3A4. (A) Purified CYP3A4 (1 μM) was divided into each of two cuvettes, and a baseline was set. Aliquots of SCH 66712 in H_2O were added to the sample cuvette, and equal volumes of H_2O were added to the reference cuvette. The increase in absorbance at lower wavelengths is due to addition of SCH 66712, which has a λ_{max} of 270 nm. (B) Plot of $\Delta A_{430-395}$ (from panel A) versus concentration of SCH 66712. K_s was determined to be $42.9 \pm 2.9 \mu\text{M}$.

dose-dependent assays with either SCH 66712 or EMTTP resulted in the loss of CYP3A4 ability to 6 β -hydroxylate testosterone (Fig. 3). Increasing the concentrations of SCH 66712 resulted in greater loss of CYP3A4 activity (Fig. 3A). Time-dependent assays with SCH 66712 resulted in a rapid loss of formation of 6 β -hydroxytestosterone with nearly complete inactivation ($\sim 90\%$) within the first 5 minutes (Fig. 3B). Addition of exogenous nucleophiles including glutathione, NAC, cyanide, and reactive oxygen species scavengers such as superoxide dismutase and catalase did not protect CYP3A4 from inactivation by SCH 66712 (Table 1).

Treatment of CYP3A4 with the structurally similar compound EMTTP also led to a concentration- and time-dependent inactivation, though the inactivation was weaker with $\sim 80\%$ loss of activity after ~ 20 minutes (Fig. 3, C and D). Addition of NAC did not protect CYP3A4 from inactivation by EMTTP; reactions with NADPH had 18% of the activity of control reactions after 12 minutes, and reactions with NADPH and NAC had 19% of the control activity. Also, a NAC conjugate of EMTTP (m/z 515) was observed in low abundance by MS in reactions with CYP3A4 and NADPH as reported previously in reactions with CYP2D6 (data not shown; Hutzler et al., 2004).

Determination of K_I and k_{inact} for SCH 66712 and EMTTP. Given that both SCH 66712 and EMTTP act as inactivators, Kitz-Wilson kinetic analysis for the determination of K_I and k_{inact} was performed. Time course data (Fig. 4, A and C) were used to estimate initial rate constants (k_{obs}) for CYP3A4 inactivation. Nonlinear regression analysis of k_{obs} and concentration of inactivators were used to determine K_I and k_{inact} (Fig. 4, B and D). Values for K_I and k_{inact} with SCH 66712 were $1.6 \pm 0.7 \mu\text{M}$ and $0.211 \pm 0.024 \text{ min}^{-1}$, respectively; K_I and k_{inact} with EMTTP were $11.8 \pm 2.6 \mu\text{M}$ and $0.044 \pm 0.004 \text{ min}^{-1}$, respectively. Efficiency of inactivation by SCH 66712 was $0.013 \mu\text{M}^{-1} \text{ min}^{-1}$ and was lower at $0.0037 \mu\text{M}^{-1} \text{ min}^{-1}$ with EMTTP. Kinetic constants are shown in Table 2.

Partition Ratio for SCH 66712 and EMTTP. The number of molecules of SCH 66712 or EMTTP metabolized per molecule of 3A4 inactivated—the partition ratio—was determined by incubation of CYP3A4 with various concentrations of SCH 66712 or EMTTP over 30 minutes to allow the inactivation to progress until essentially complete. The percentage of the activity remaining was plotted as a function of the molar ratio of inactivator to CYP3A4. The turnover number (partition ratio + 1) was estimated from the intercept of the linear regression line obtained from the lower ratios of inactivator to CYP3A4 as described previously elsewhere (Silverman, 1988). With this method, the turnover number for SCH 66712 was 12, and the partition ratio was 11 (Fig. 5). The less potent inactivator EMTTP showed a partition ratio of 94.

Analysis of Heme. Heme adduction was examined by HPLC analysis of heme at 405 nm. Incubation of CYP3A4 with SCH 66712 in the presence of NADPH generated only $<10\%$ loss of native heme as compared with controls with no SCH 66712 or no NADPH (Supplemental Fig. 1). Furthermore, MS analysis of the heme showed only m/z 616 with no peaks at potential adducted masses (data not shown).

Covalent Binding of Inactivators to CYP3A4. Given the lack of heme adducts, CYP3A4 apoprotein was analyzed for the presence of protein adducts. CYP3A4 was treated with SCH 66712 or EMTTP and analyzed by LC/MS as described in *Materials and Methods*. Chromatograms showed clear separation of cytochrome b_5 , clipped reductase, reductase, CYP3A4, and lipids (Fig. 6, A, D, and G). Deconvoluted masses of clipped reductase, reductase, and lipids were as expected at 70,363 Da, 77,727 Da, and 622/1243 Da, respectively (data not shown).

In the absence of both NADPH and SCH 66712, the CYP3A4 mass spectrum deconvoluted to 56,952 Da (Fig. 6, B and C). Addition of

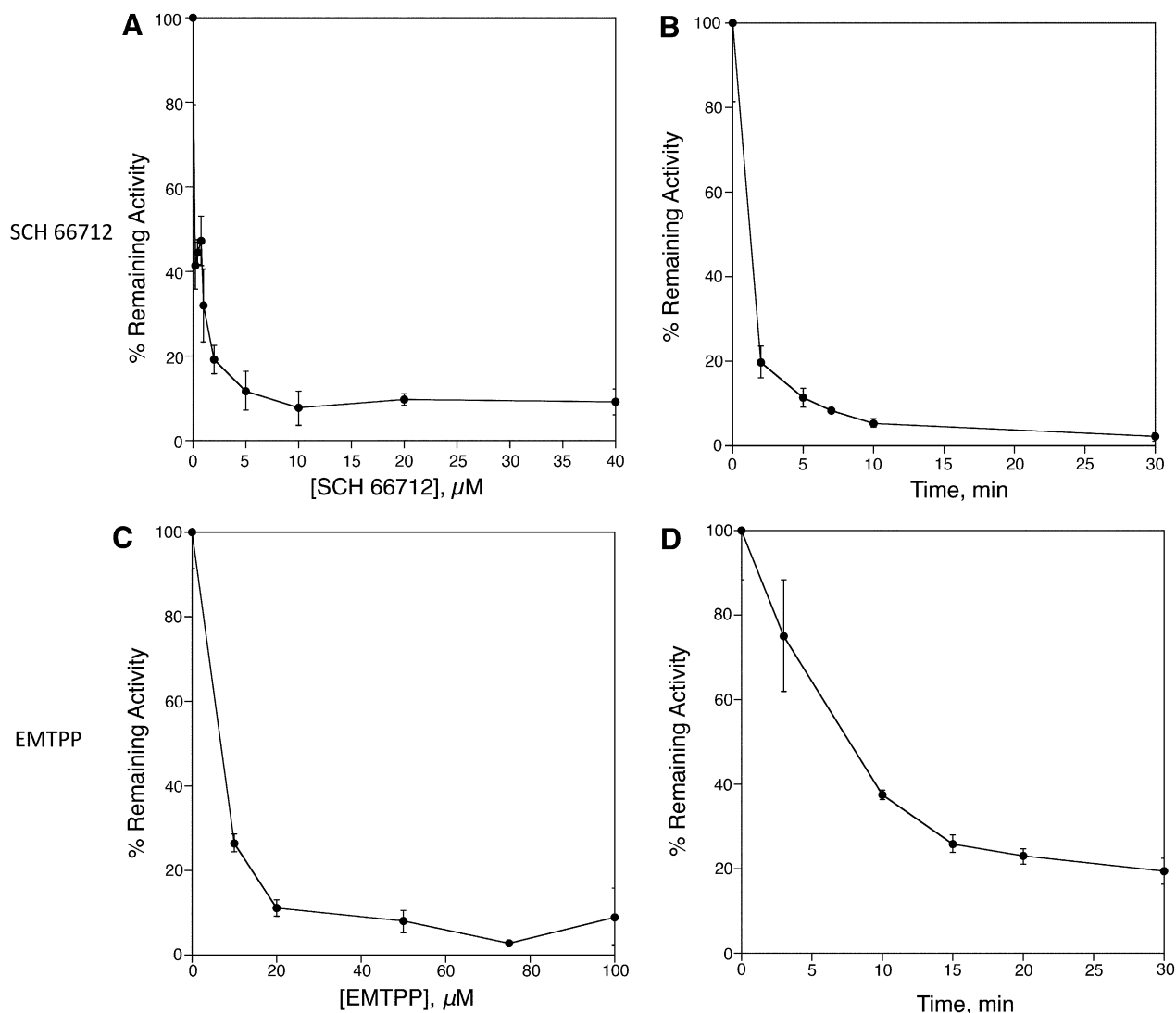


Fig. 3. Time- and concentration-dependent inactivation of CYP3A4 by SCH 66712 and EMTTP. (A) Concentration-dependent inactivation by SCH 66712 in 20-minute reactions. (B) Time-dependent inactivation by SCH 66712 (16 μM). (C) Concentration-dependent inactivation by EMTTP in 20-minute reactions. (D) Time-dependent inactivation by EMTTP (20 μM).

NADPH increased the noise and lowered the signal abundance by an order of magnitude in the mass spectrum (Fig. 6E), but showed a consistent CYP3A4 deconvoluted mass of 56,958 Da (Fig. 6F). The presence of SCH 66712 and NADPH also resulted in more noise and lower signal in the mass spectrum (Fig. 6H). Deconvolution of the SCH 66712-treated sample, however, resulted in the appearance of an adducted protein mass at 57,284 Da as well as the nonadducted protein peak with mass of 56,957 Da (Fig. 6I). The difference between the parent CYP3A4 peak and adducted peak was 327 Da, approximately the mass of one SCH 66712 molecule (338 Da). The experiment was repeated three times with the difference in adducted mass peak varying between 327 to 348 Da, with an average difference of 338 Da; these values are consistent with adduction by one SCH 66712 molecule. These differences are within the mass accuracy of the LXQ instrument combined with the limits of the ProMass deconvolution software and are similar to differences seen by other groups (Regal et al., 2000; Jushchyshyn et al., 2003; Bateman et al., 2004; Hutzler et al., 2004; Lin et al., 2005, 2009, 2012; Zhang et al., 2011). EMTTP also adducted CYP3A4 with mass consistent with monoadduction by EMTTP

(353 Da; data not shown). These results also support a 1:1 binding stoichiometry between CYP3A4 and SCH 66712 or EMTTP.

As a validation assay of the mass spectrum and deconvolution data, CYP3A4 was treated with the cysteine alkylating agent iodoacetamide that can form zero, one, or two alkyl adducts on solvent accessible

TABLE 1
Inactivation of CYP3A4 by SCH 66712 is not prevented by trapping agents

Assay Components ^a	% Activity
No NADPH—Control, SCH 66712	100
NADPH, SCH 66712	15
NADPH, SCH 66712, GSH (10 mM)	13
NADPH, SCH 66712, NAC (10 mM)	18
NADPH, SCH 66712, SOD (1 U/ μl)	10
NADPH, SCH 66712, catalase (0.05 $\mu\text{g}/\mu\text{l}$)	9
NADPH, SCH 66712, cyanide (2 mM)	15

GSH, glutathione; SOD, superoxide dismutase.

^aAll reactions contained 16 μM SCH 66712 and were performed for 12 minutes.

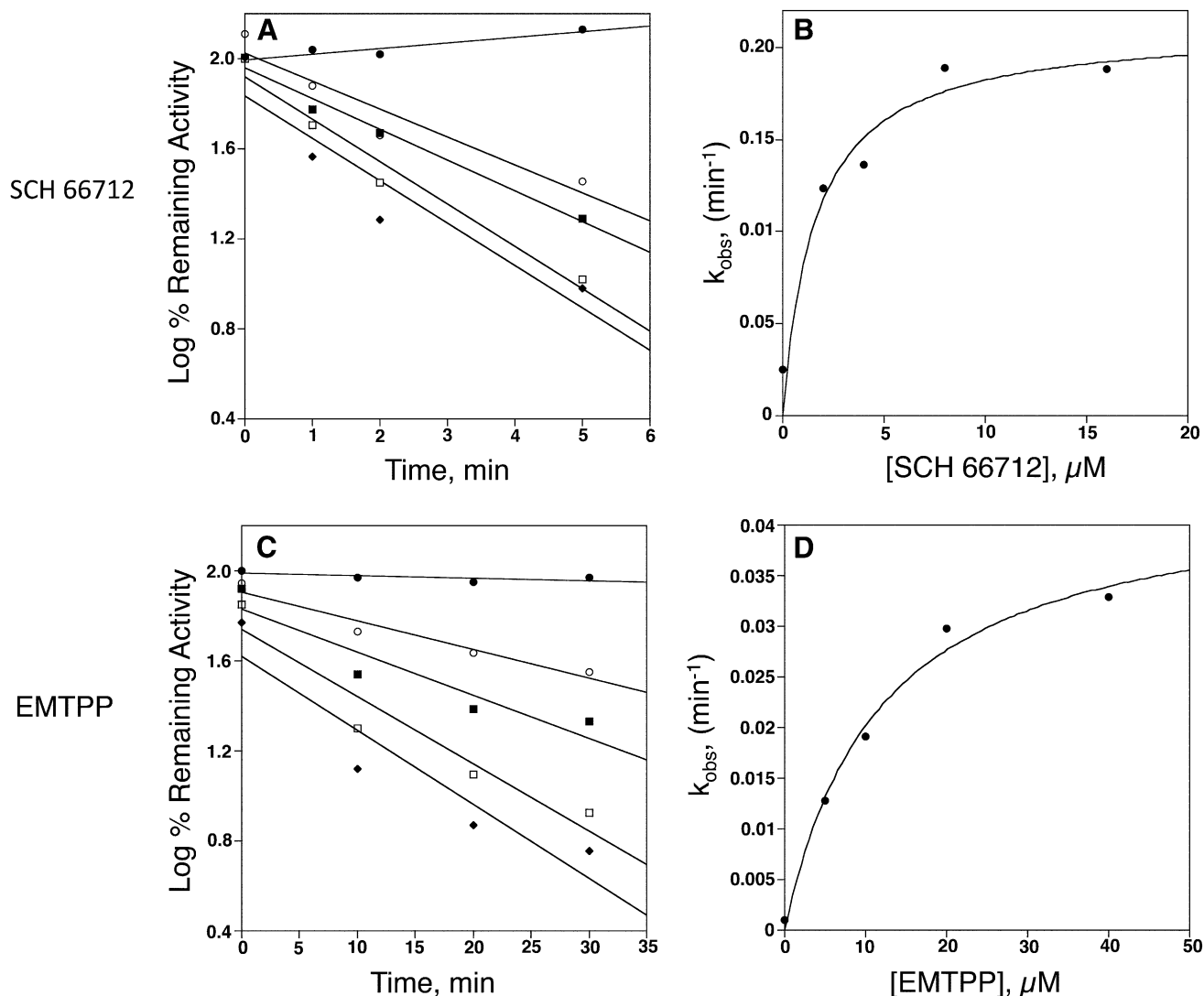


Fig. 4. Determination of K_1 and k_{inact} for the inactivation of CYP3A4 by SCH 66712 and EMTTP. (A) Inactivation of CYP3A4 by SCH 66712 (0, 2, 4, 8, and 16 μM). (B) K_1 and k_{inact} for the inactivation of CYP3A4 by SCH 66712 were $1.6 \pm 0.7 \mu\text{M}$ and $0.211 \pm 0.024 \text{ min}^{-1}$, respectively, as determined using Kitz-Wilson analysis and nonlinear regression. Efficiency of inactivation k_{inact}/K_1 was $0.013 \mu\text{M}^{-1}\text{min}^{-1}$. (C) Inactivation of CYP3A4 by EMTTP (0, 5, 10, 20, and 40 μM). (D) K_1 and k_{inact} for the inactivation of CYP3A4 by EMTTP were $11.8 \pm 2.6 \mu\text{M}$ and $0.044 \pm 0.004 \text{ min}^{-1}$, respectively, as determined using Kitz-Wilson analysis and nonlinear regression. Efficiency of inactivation k_{inact}/K_1 was $0.0037 \mu\text{M}^{-1}\text{min}^{-1}$.

cysteine residues in CYP3A4 (Baer et al., 2007). Treatment of CYP3A4 with iodoacetamide was consistent with the formation of two adducts as indicated by the difference of 117 Da in deconvoluted mass of CYP3A4 in the absence (56,953 Da) and presence (57,070 Da) of iodoacetamide (Supplemental Fig. 2).

Metabolism of SCH 66712. Previous studies in our group identified four mono-oxygenated metabolites of SCH 66712 in the presence of NADPH with molecular ion at m/z 355. The four products were formed in varying proportions by CYP2D6, CYP2C9, CYP2C19, and CYP3A4 (Nagy et al., 2011; Supplemental Figs. 3A and 4A; and unpublished data). No other metabolites were detected (Nagy et al., 2011; and unpublished data). Collision-induced dissociation fragmentation showed that one of the four products, peak 1, was mono-oxygenated on the phenyl ring end of the molecule (Supplemental Fig. 3B and Nagy et al., 2011). The other three products were shown through collision-induced dissociation to be oxygenated on the piperazine or the heteroaromatic ring (Supplemental Fig. 3) (Nagy et al., 2011).

Because both carbon and nitrogen oxygenation are possible products of metabolism, in the present study we treated the metabolites formed with TiCl_3 to further identify the sites of metabolism. TiCl_3 reverses N-hydroxylations but not C-hydroxylations (Seto and Guengerich, 1993; Kulanthaivel et al., 2004). Treatment of the four metabolites with TiCl_3 resulted in specific loss of only one product peak (peak 3) in the MS, indicating that one site of metabolism is a nitrogen on the heteroaromatic ring end of the molecule (Supplemental Fig. 4). Product

TABLE 2

Kinetic constants for inactivation of CYP3A4 by SCH 66712 and EMTTP

Inactivator	K_1 μM	k_{inact} min^{-1}	k_{inact}/K_1 $\text{min}^{-1} \mu\text{M}^{-1}$
SCH 66712	1.6 ± 0.7	0.211 ± 0.024	0.013
EMTTP	11.8 ± 2.6	0.044 ± 0.004	0.0037

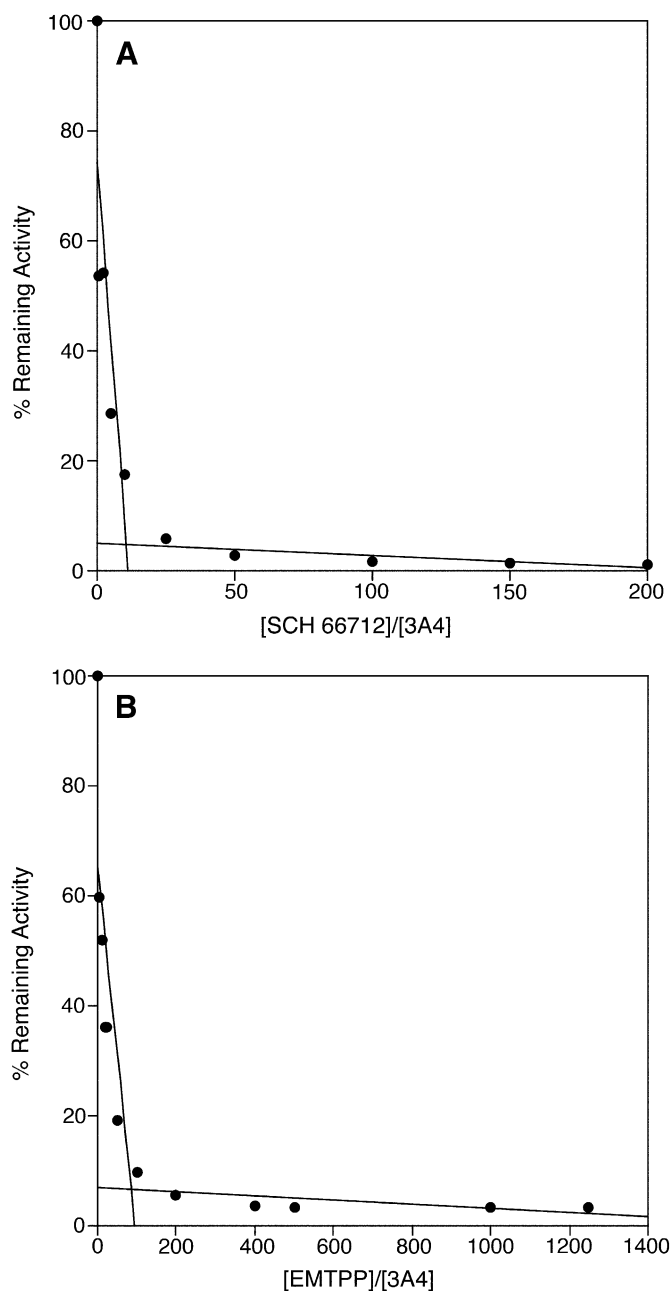


Fig. 5. Partition ratio for SCH 66712 inactivation of CYP3A4. CYP3A4 was incubated with varying concentrations of SCH 66712 (A) or EMTTP (B) for 30 minutes to allow for complete inactivation. With SCH 66712, the turnover number was 12, and the partition ratio was estimated to be 11. With EMTTP, the turnover number was 95, and the partition ratio was estimated to be 94.

peak 2 was lost in the control reactions treated with HCl alone and must be acid liable (other groups have seen similar issues upon acid treatment, e.g., Kulanthaivel et al., 2004). The mass spectra of product peaks 1 and 4 were unaffected by the addition of HCl or TiCl_3 and are presumed therefore to be carbon hydroxylations.

MS^n data and TiCl_3 data were combined with SMARTCyp and RS Predictor predictions of sites of metabolism on SCH 66712 (Supplemental Table 1). The prediction software was more accurate with CYP2D6 sites of metabolism than for CYP3A4 though both software programs performed similarly.

Metabolism of EMTTP. Incubation of CYP3A4 with EMTTP and NADPH resulted in the formation of eight mono-oxygenated product

peaks with molecular ion m/z at 370 (Supplemental Fig. 5). Four of the metabolites, product peaks 4, 5, 7, and 8, represent mono-oxygenation on the imidazole end of the molecule whereas the other four product peaks, 1, 2, 3, and 6, represent mono-oxygenation on the piperazine/heteroaromatic end of the molecule (Supplemental Fig. 5). MS^3 combined with TiCl_3 analysis confirmed mono-oxygenation at some sites, including on the ethyl substituent of the imidazole ring, mono-oxygenation on the imidazole ring (analysis by TiCl_3 treatment was inclusive as to C- or N-hydroxylation), and mono-oxygenation on the N of the heteroaromatic ring (Supplemental Table 1 and data not shown). No dehydrogenation or other metabolites were observed. Previous analysis of metabolism of EMTTP by CYP2D6 showed only two mono-oxygenation products (m/z 370) and one dehydrogenation product (m/z 351) (Hutzler et al., 2004).

Molecular Modeling. A series of molecular modeling studies were performed to better understand the metabolism of SCH 66712 and EMTTP that would lead to inactivation of CYP3A4.

With SCH 66712, the lowest energy and most common docking poses were with the phenyl ring of SCH 66712 in stacking geometry with Phe304 (Supplemental Fig. 6A). This placed the imidazole group and methylene closest to the heme iron at a distance of ~ 4.6 Å. An additional orientation observed was with the heteroaromatic ring parallel to the heme group at ~ 3.3 Å above the heme. In this configuration, the phenyl group pointed to the phenylalanine cluster in the roof the active site of CYP3A4 at ~ 4.0 Å from Phe213 and Phe215 (Supplemental Fig. 6A). Binding free energies for SCH 66712 docking ranged from -9.4 kcal/mol to -8.3 kcal/mol.

Docking experiments with EMTTP resulted in lowest energy conformations with the CF_3 group pointing toward Phe304 and placement of the six-membered heteroaromatic ring closest to the heme iron at ~ 4.4 Å (Supplemental Fig. 6B). In the other major orientation, the ethyl group of the imidazole ring was pointing toward Phe304, and the methylene group connecting the imidazole and piperazine rings was closest to the heme iron at ~ 4.2 Å. Stacking interactions between phenylalanine residues in CYP3A4 and aromatic rings in EMTTP were not observed in any of the docking results (data not shown). Binding free energies for EMTTP docking were weaker and ranged from -8.2 kcal/mol to -7.1 kcal/mol.

Discussion

The inactivation of CYP3A4 by SCH 66712 and EMTTP was concentration, time, and NADPH dependent. Inactivation by SCH 66712 proceeded with k_{inact} of 0.211 min^{-1} and K_I of $1.60 \mu\text{M}$ and overall efficiency of inactivation of $0.013 \mu\text{M}^{-1}\text{min}^{-1}$. EMTTP was a weaker inactivator with k_{inact} of 0.044 min^{-1} and K_I of $11.8 \mu\text{M}$ and overall efficiency of inactivation of $0.0037 \mu\text{M}^{-1}\text{min}^{-1}$. The partition ratios for inactivation of CYP3A4 by SCH 66712 and EMTTP were 11 and 94, respectively, confirming that SCH 66712 is a more potent inactivator. Mass spectral analysis of CYP3A4 showed 1:1 binding stoichiometry for both SCH 66712 and EMTTP with no heme modifications. These results support CYP3A4 apoprotein adduction by both inactivators.

Metabolism of SCH 66712 by CYP3A4 produced the same metabolites as CYP2D6 as we previously reported elsewhere (Nagy et al., 2011). However, the proportions of products produced were different. With CYP3A4 and SCH 66712, product peak 4, mono-oxygenation on the piperazine/heteroaromatic ring end of the molecule, was in highest abundance (Supplemental Fig. 3). Using TiCl_3 treatment of the SCH 66712 metabolites, product peak 4 was confirmed to be a carbon hydroxylation, not a nitrogen hydroxylation, because TiCl_3 reverses nitrogen hydroxylations (Seto and

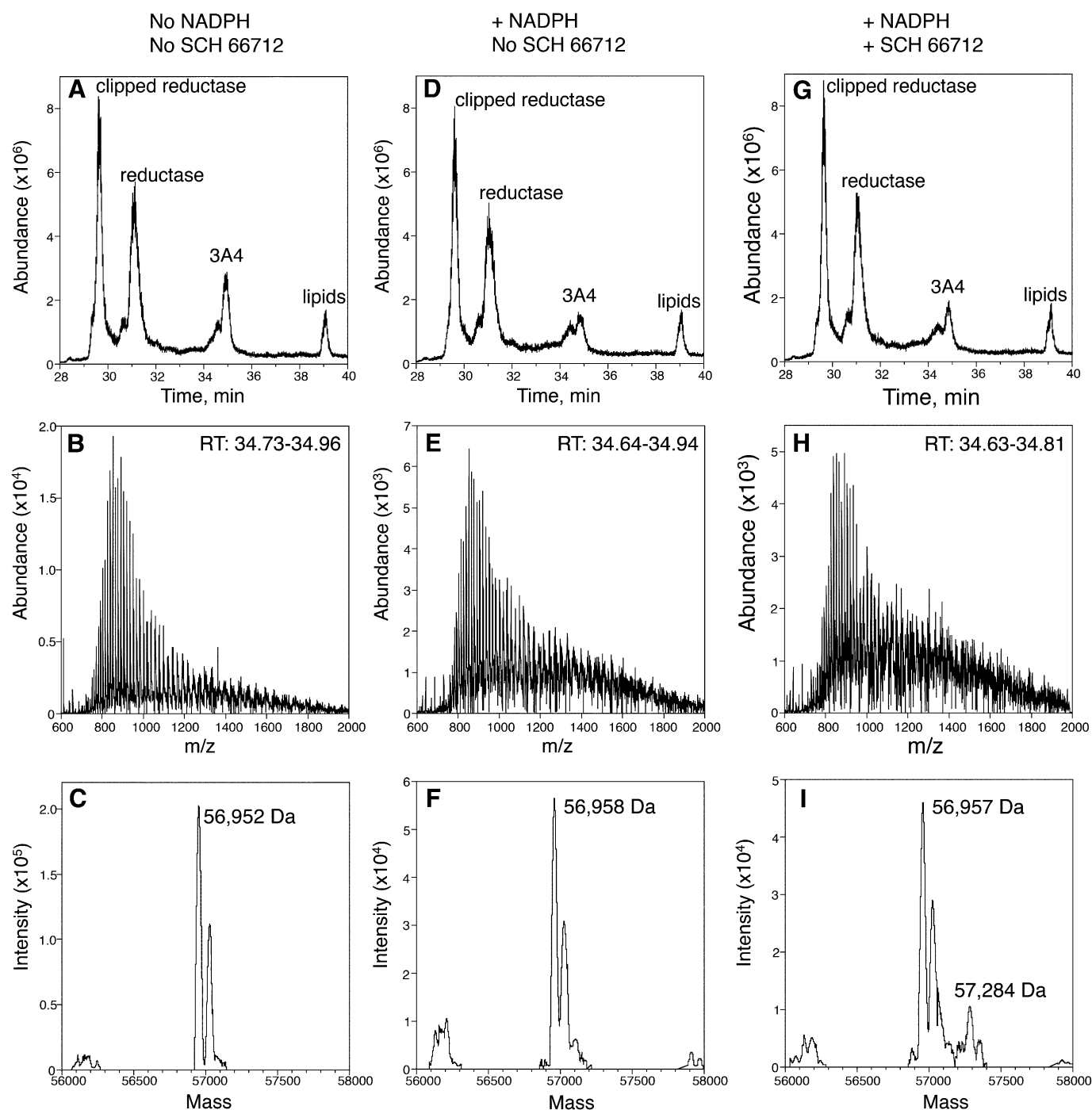


Fig. 6. LC-ESI-MS analysis of CYP3A4 incubated with SCH 66712. (A) Chromatogram of reaction with no NADPH and no SCH 66712. (B) ESI-MS of recombinant CYP3A4 from panel (A). (C) Deconvolution of MS in panel (B) yielded mass of 56,952 Da for CYP3A4. (D) Chromatogram of reaction with NADPH but without SCH 66712. (E) ESI-MS of recombinant CYP3A4 from panel (D). The addition of NADPH resulted in loss of signal and increased background noise. (F) Deconvolution of MS in panel (E) yielded mass of 56,958 Da for CYP3A4. (G) Chromatogram of reaction with NADPH and with SCH 66712. (H) ESI-MS of recombinant CYP3A4 from panel (G). (I) Deconvolution of MS in panel (H) yielded mass of 56,957 Da for nonadducted CYP3A4 and mass of 57,284 Da for adducted CYP3A4. The mass increase for the adducted form is consistent with mono-adduction of CYP3A4 by SCH 66712. Chromatograms (A), (D), and (G) show separation of reconstituted system by HPLC and elution of clipped reductase, reductase, CYP3A4, and lipids.

Guengerich, 1993; Kulanthaivel et al., 2004; Livezey et al., 2014) (Supplemental Fig. 4).

Compared with CYP2D6, CYP3A4 produced many additional mono-oxygenation products of EMTTP (Supplemental Fig. 5; Hutzler et al., 2004). Sites of metabolism were confirmed on each major functional group including the ethyl group, imidazole ring, piperazine ring, and heteroaromatic ring (Supplemental Table 1 and Supplemental Fig. 5).

For both SCH 66712 and EMTTP, observed docking orientations in the active site of CYP3A4 were consistent with the multiple sites of metabolism observed in MS experiments. Both inactivators are small substrates for CYP3A4, and there was considerable room for docking of the inactivators within the active site. Interaction between the phenyl ring of SCH 66712 and Phe304 perhaps could provide a stabilizing interaction that would lead to fewer products formed, as observed in

metabolite assays (Supplemental Fig. 3A). In metabolite assays, the major SCH 66712 product formed by CYP3A4 was a C-mono-oxygenation on the piperazine/heteroaromatic ring end of SCH 66712—the end of the molecule that would be positioned best for metabolism based on the docking experiment (Supplemental Fig. 6A). Conversely, EMTTP did not form significant stabilizing interactions that could hold EMTTP in a particular orientation for metabolism, possibly explaining the large variety of mono-oxygenation products formed from EMTTP by CYP3A4. Furthermore, the binding free energies from docking experiments were less favorable for EMTTP than for SCH 66712.

There are many MBIs of CYP3A4 reported in the literature, but only a few of CYP2D6, including only two known apoprotein adductors, SCH 66712 and EMTTP. Inactivation of CYP2D6 by SCH 66712 was more potent than inactivation of CYP3A4, with a partition ratio of 3 and k_{inact} and K_I of 0.032 min^{-1} and $0.55 \text{ }\mu\text{M}$, respectively (Nagy et al., 2011). However, inactivation by EMTTP was similar for both CYP2D6 and CYP3A4 (partition ratios of 99 and 94 for CYP2D6 and CYP3A4, respectively; and k_{inact} and K_I values of 0.09 min^{-1} and $5.5 \text{ }\mu\text{M}$ for CYP2D6 versus 0.044 min^{-1} and $11.8 \text{ }\mu\text{M}$ for CYP3A4). CYP2D6 inactivation by SCH 66712 and EMTTP also proceeded with 1:1 binding stoichiometries and no protection from inactivation by free radical scavengers (Palamanda et al., 2001; Hutzler et al., 2004; Nagy et al., 2011).

SCH 66712 and EMTTP are structurally related with piperazine rings, substituted imidazoles, and fluorinated heteroaromatic rings. To our knowledge, there have been no reports of potent MBI of CYP2D6 and CYP3A4 by the same inactivator [though there are conflicting reports regarding inactivation by tamoxifen (Sridar et al., 2002; Zhao et al., 2002)]. Part of the lack of dual inactivators of both CYP3A4 and CYP2D6 is the difference in the presence of potential requisite nucleophile(s) in the active site. For instance, Vandenbrink et al. (2012) have shown that while raloxifene is a potent inactivator of CYP3A4, it does not inactivate CYP2D6. They further showed by structural analysis that CYP2D6 lacks cysteine residues in the quadrant most likely to interact with raloxifene and other soft-electrophile inactivators. It seems likely that SCH 66712 and EMTTP are not adducting at a cysteine since both 2D6 and 3A4 experience inactivation.

We previously proposed that a quinone could be the reactive electrophile in the mechanism of CYP2D6 inactivation by SCH 66712 (Nagy et al., 2011). However, we were unable to isolate a thiol-adduct in the presence of NAC or glutathione with SCH 66712. In contrast, we were able to observe an NAC-EMTTP conjugate in reactions with CYP3A4 as did Hutzler et al. (2004) with CYP2D6. Hutzler et al. (2004) showed by NMR that the electrophile of EMTTP that reacted with NAC had formed on the methylene group of the ethyl substituent of the imidazole ring. However, they were unable to identify the amino acid target in CYP2D6.

In our molecular models and those of others, it is not clear that a thiol such as cysteine would be available in CYP2D6 for inactivation on the distal side (Vandenbrink et al., 2012). It may be that the ethyl substituent of EMTTP is not the source of the reactive electrophile that leads to inactivation, as several other metabolites were also formed by reactions at other sites in EMTTP and in SCH 66712 by both CYP2D6 and CYP3A4. Furthermore, in activity assays in our present study with CYP3A4, the addition of NAC did not prevent inactivation by EMTTP, though a NAC-EMTTP conjugate was captured by MS. No conjugates of SCH 66712 were observed in reactions with CYP3A4 or previous studies with CYP2D6 (Nagy et al., 2011). Future studies aimed at identifying the exact structural characteristic(s) of SCH 66712 (and EMTTP) that plays a role in the covalent binding of SCH66712 to CYP3A4 and CYP2D6, and the specific location of the covalent adduction to the P450 enzymes, will provide great insight to drug design. Comparing the

similarities and differences between inactivation of CYP2D6 and CYP3A4 by SCH66712 will additionally provide insight into enzyme function and specificity.

Conclusion

The inactivation of CYP3A4 and CYP2D6 is of great clinical significance because together they are responsible for the metabolism of 70% of all pharmaceutical drugs currently on the market. Mechanism-based inactivation of P450s is of particular interest because of its irreversible nature and dependence on enzyme catalysis. SCH 66712 and EMTTP have been previously identified as a MBI of CYP2D6, and our study shows SCH 66712 and EMTTP to be inactivators of CYP3A4 as well.

Acknowledgments

The authors thank Dr. F.P. Guengerich for making this collaboration possible, Drs. P. Hollenberg, H. Zhang, and A. Venter, and G. Cavey for helpful comments, Dr. M.V. Martin for preparing purified recombinant P450 NADPH-reductase and cytochrome b_5 , and Dr. Mark Hail of Novatia for assistance with ProMass software.

Authorship Contributions

Participated in research design: Bolles, Fujiwara, Nomeir, Furge.
Conducted experiments: Bolles, Fujiwara, Briggs, Furge.
Contributed new reagents or analytic tools: Nomeir.
Performed data analysis: Bolles, Fujiwara, Furge.
Wrote or contributed to the writing of the manuscript: Bolles, Fujiwara, Briggs, Nomeir, Furge.

References

- Alvarez-Diez TM and Zheng J (2004) Detection of glutathione conjugates derived from 4-ipomeanol metabolism in bile of rats by liquid chromatography-tandem mass spectrometry. *Drug Metab Dispos* **32**:1345–1250.
- Baer BR, Wienkers LC, and Rock DA (2007) Time-dependent inactivation of P450 3A4 by raloxifene: identification of Cys239 as the site of apoprotein alkylation. *Chem Res Toxicol* **20**: 954–964.
- Bateman KP, Baker J, Wilke M, Lee J, Leriche T, Seto C, Day S, Chaurat N, Ouellet M, and Nicoll-Griffith DA (2004) Detection of covalent adducts to cytochrome P450 3A4 using liquid chromatography mass spectrometry. *Chem Res Toxicol* **17**:1356–1361.
- Chen Q, Ngui JS, Doss GA, Wang RW, Cai X, DiNinno FP, Blizzard TA, Hammond ML, Stearns RA, and Evans DC, et al. (2002) Cytochrome P450 3A4-mediated bioactivation of raloxifene: irreversible enzyme inhibition and thiol adduct formation. *Chem Res Toxicol* **15**:907–914.
- Correia MA and Ortiz de Montellano PR (2005) Inhibition of cytochrome P450 enzymes, in *Cytochrome P450: Structure, Mechanism, and Biochemistry* (Ortiz de Montellano PR ed), pp 247–322. Kluwer Academic/Plenum, New York.
- Ekkroos M and Sjögren T (2006) Structural basis for ligand promiscuity in cytochrome P450 3A4. *Proc Natl Acad Sci USA* **103**:13682–13687.
- Emsley P and Cowtan K (2004) Coot: model-building tools for molecular graphics. *Acta Crystallogr D Biol Crystallogr* **60**:2126–2132.
- Gillam EMJ, Baba T, Kim B-R, Ohmori S, and Guengerich FP (1993) Expression of modified human cytochrome P450 3A4 in *Escherichia coli* and purification and reconstitution of the enzyme. *Arch Biochem Biophys* **305**:123–131.
- Gillam EMJ, Guo Z, Ueng Y-F, Yamazaki H, Cock I, Reilly PEB, Hooper WD, and Guengerich FP (1995) Expression of cytochrome P450 3A5 in *Escherichia coli*: effects of 5' modification, purification, spectral characterization, reconstitution conditions, and catalytic activities. *Arch Biochem Biophys* **317**:374–384.
- Guengerich FP (2003) Cytochromes P450, drugs, and diseases. *Mol Interv* **3**:194–204.
- Guengerich FP (2005) Human cytochrome P450 enzymes, in *Cytochrome P450: Structure, Mechanism, and Biochemistry* (Ortiz de Montellano PR ed), pp 377–530. Kluwer Academic/Plenum, New York.
- He K, Iyer KR, Hayes RN, Sinz MW, Woolf TF, and Hollenberg PF (1998) Inactivation of cytochrome P450 3A4 by bergamotol, a component of grapefruit juice. *Chem Res Toxicol* **11**: 252–259.
- Henne KR, Tran TB, Vandenbrink BM, Rock DA, Aidarani DK, Subramanian R, Mason AK, Stresser DM, Teffera Y, and Wong SG, et al. (2012) Sequential metabolism of AMG 487, a novel CXCR3 antagonist, results in formation of quinone reactive metabolites that covalently modify CYP3A4 Cys239 and cause time-dependent inhibition of the enzyme. *Drug Metab Dispos* **40**:1429–1440.
- Hollenberg PF, Kent UM, and Bumpus NN (2008) Mechanism-based inactivation of human cytochromes p450s: experimental characterization, reactive intermediates, and clinical implications. *Chem Res Toxicol* **21**:189–205.
- Holmans PL, Shet MS, Martin-Wixtrom CA, Fisher CW, and Estabrook RW (1994) The high-level expression in *Escherichia coli* of the membrane-bound form of human and rat cytochrome b_5 and studies on their mechanism of function. *Arch Biochem Biophys* **312**:554–565.
- Huey R, Morris GM, Olson AJ, and Goodsell DS (2007) A semiempirical free energy force field with charge-based desolvation. *J Comput Chem* **28**:1145–1152.

- Hutzler JM, Steenwyk RC, Smith EB, Walker GS, and Wienkers LC (2004) Mechanism-based inactivation of cytochrome P450 2D6 by 1-[(2-ethyl-4-methyl-1H-imidazol-5-yl)methyl]-4-[4-(trifluoromethyl)-2-pyridinyl]piperazine: kinetic characterization and evidence for apoprotein adduction. *Chem Res Toxicol* **17**:174–184.
- Jushchyshyn MI, Kent UM, and Hollenberg PF (2003) The mechanism-based inactivation of human cytochrome P450 2B6 by phenylclidine. *Drug Metab Dispos* **31**:46–52.
- Kulanthaivel P, Parbuchi RJ, Davidson RS, Yi P, Renner GA, Mattiuz EL, Hadden CE, Goodwin LA, and Ehlhardt WJ (2004) Selective reduction of N-oxides to amines: application to drug metabolism. *Drug Metab Dispos* **32**:966–972.
- Lin HL, Kanaan C, and Hollenberg PF (2012) Identification of the residue in human CYP3A4 that is covalently modified by bergamottin and the reactive intermediate that contributes to the grapefruit juice effect. *Drug Metab Dispos* **40**:998–1006.
- Lin HL, Kent UM, and Hollenberg PF (2002) Mechanism-based inactivation of cytochrome P450 3A4 by 17 alpha-ethynylestradiol: evidence for heme destruction and covalent binding to protein. *J Pharmacol Exp Ther* **301**:160–167.
- Lin HL, Kent UM, and Hollenberg PF (2005) The grapefruit juice effect is not limited to cytochrome P450 (P450) 3A4: evidence for bergamottin-dependent inactivation, heme destruction, and covalent binding to protein in P450s 2B6 and 3A5. *J Pharmacol Exp Ther* **313**:154–164.
- Lin HL, Zhang H, Noon KR, and Hollenberg PF (2009) Mechanism-based inactivation of CYP2B1 and its F-helix mutant by two tert-butyl acetylenic compounds: covalent modification of prosthetic heme versus apoprotein. *J Pharmacol Exp Ther* **331**:392–403.
- Livezey MR, Briggs ED, Bolles AK, Nagy LD, Fujiwara R, and Furge LL (2014) Metoclopramide is metabolized by CYP2D6 and is a reversible inhibitor, but not inactivator, of CYP2D6. *Xenobiotica* **44**:309–319.
- Livezey M, Nagy LD, Diffenderfer LE, Arthur EJ, Hsi DJ, Holton JM, and Furge LL (2012) Molecular analysis and modeling of inactivation of human CYP2D6 by four mechanism based inactivators. *Drug Metab Lett* **6**:7–14.
- Morris GM, Goodsell DS, Halliday RS, Huey R, Hart WE, Belew RK, and Olson AJ (1998) Automated docking using a Lamarckian genetic algorithm and empirical binding free energy function. *J Comput Chem* **19**:1639–1662 DOI: 10.1002/(SICI)1096-987X(19981115)19:14<1639::AID-JCC10>3.0.CO;2-B.
- Nagy LD, Mooney CS, Diffenderfer LE, Hsi DJ, Butler BF, Arthur EJ, Fletke KJ, Palamanda JR, Nomeir AA, and Furge LL (2011) Substituted imidazole of 5-fluoro-2-[4-[(2-phenyl-1H-imidazol-5-yl)methyl]-1-piperazinyl]pyrimidine Inactivates cytochrome P450 2D6 by protein adduction. *Drug Metab Dispos* **39**:974–983.
- Palamanda JR, Casciano CN, Norton LA, Clement RP, Favreau LV, Lin C, and Nomeir AA (2001) Mechanism-based inactivation of CYP2D6 by 5-fluoro-2-[4-[(2-phenyl-1H-imidazol-5-yl)methyl]-1-piperazinyl]pyrimidine. *Drug Metab Dispos* **29**:863–867.
- Regal KA, Schrag ML, Kent UM, Wienkers LC, and Hollenberg PF (2000) Mechanism-based inactivation of cytochrome P450 2B1 by 7-ethynylcoumarin: verification of apo-P450 adduction by electrospray ion trap mass spectrometry. *Chem Res Toxicol* **13**:262–270.
- Rowland P, Blaney FE, Smyth MG, Jones JJ, Leydon VR, Oxbrow AK, Lewis CJ, Tennant MG, Modi S, and Eggleston DS, et al. (2006) Crystal structure of human cytochrome P450 2D6. *J Biol Chem* **281**:7614–7622.
- Rydberg P, Gloriam DE, and Olsen L (2010) The SMARTCyp cytochrome P450 metabolism prediction server. *Bioinformatics* **26**:2988–2989.
- Rydberg P and Olsen L (2012) Predicting drug metabolism by cytochrome P450 2C9: comparison with the 2D6 and 3A4 isoforms. *ChemMedChem* **7**:1202–1209.
- Seto Y and Guengerich FP (1993) Partitioning between N-dealkylation and N-oxygenation in the oxidation of N,N-dialkylarylamines catalyzed by cytochrome P450 2B1. *J Biol Chem* **268**:9986–9997.
- Sevrioukova IF and Poulos TL (2010) Structure and mechanism of the complex between cytochrome P4503A4 and ritonavir. *Proc Natl Acad Sci USA* **107**:18422–18427.
- Shahrokh K, Orendt A, Yost GS, and Cheatham TE, 3rd (2012) Quantum mechanically derived AMBER-compatible heme parameters for various states of the cytochrome P450 catalytic cycle. *J Comput Chem* **33**:119–133.
- Shen AL, Porter TD, Wilson TE, and Kasper CB (1989) Structural analysis of the FMN binding domain of NADPH-cytochrome P-450 oxidoreductase by site-directed mutagenesis. *J Biol Chem* **264**:7584–7589.
- Silverman RB (1988) *Mechanism-based Enzyme Inactivation: Chemistry and Enzymology*, CRC Press, Boca Raton, FL.
- Sohl CD, Cheng Q, and Guengerich FP (2009) Chromatographic assays of drug oxidation by human cytochrome P450 3A4. *Nat Protoc* **4**:1252–1257.
- Sridar C, Kent UM, Notley LM, Gillam EM, and Hollenberg PF (2002) Effect of tamoxifen on the enzymatic activity of human cytochrome CYP2B6. *J Pharmacol Exp Ther* **301**:945–952.
- Teng WC, Oh JW, New LS, Wahlin MD, Nelson SD, Ho HK, and Chan EC (2010) Mechanism-based inactivation of cytochrome P450 3A4 by lapatinib. *Mol Pharmacol* **78**:693–703.
- VandenBrink BM, Davis JA, Pearson JT, Foti RS, Wienkers LC, and Rock DA (2012) Cytochrome p450 architecture and cysteine nucleophile placement impact raloxifene-mediated mechanism-based inactivation. *Mol Pharmacol* **82**:835–842.
- Yukinaga H, Takami T, Shioyama SH, Tozuka Z, Masumoto H, Okazaki O, and Sudo K (2007) Identification of cytochrome P450 3A4 modification site with reactive metabolite using linear ion trap-Fourier transform mass spectrometry. *Chem Res Toxicol* **20**:1373–1378.
- Zaretski J, Rydberg P, Bergeron C, Bennett KP, Olsen L, and Breneman CM (2012) RS-Predictor models augmented with SMARTCyp reactivities: robust metabolic regioselectivity predictions for nine CYP isozymes. *J Chem Inf Model* **52**:1637–1659.
- Zhang H, Amunugama H, Ney S, Cooper N, and Hollenberg PF (2011) Mechanism-based inactivation of human cytochrome P450 2B6 by clopidogrel: involvement of both covalent modification of cysteinyl residue 475 and loss of heme. *Mol Pharmacol* **80**:839–847.
- Zhao XJ, Jones DR, Wang YH, Grimm SW, and Hall SD (2002) Reversible and irreversible inhibition of CYP3A enzymes by tamoxifen and metabolites. *Xenobiotica* **32**:863–878.
- Zhou S, Yung Chan S, Cher Goh B, Chan E, Duan W, Huang M, and McLeod HL (2005) Mechanism-based inhibition of cytochrome P450 3A4 by therapeutic drugs. *Clin Pharmacokinetics* **44**:279–304.

Address correspondence to: Laura Lowe Furge, Department of Chemistry, Kalamazoo College, 1200 Academy Street, Kalamazoo, MI 49006. E-mail: laura.furge@kzoo.edu.
